Journal of Nuclear Materials 111 & 112 (1982) 554–559
North-Holland Publishing Company

DYNAMICS OF MELTING, EVAPORATION, AND RESOLIDIFICATION OF MATERIALS EXPOSED TO PLASMA DISRUPTIONS

A.M. HASSANEIN, G.L. KULCINSKI and W.G. WOLFER

Fusion Engineering Program, Nuclear Engineering Department, University of Wisconsin, Madison, Wisconsin 53706, USA

First wall components exposed to a high energy flux during a plasma disruption experience a sequence of processes which consists of rapid heating, melting, intense evaporation, resolidification, and cool-down. The dynamics of all these processes has an impact on both the melt layer stability and the thermal stress cycle in the component of the first wall that stays solid. The detailed time history of the temperature distribution is accurately computed by solving a two-moving-boundary problem. The time behavior of the melt layer thickness for both stainless steel and molybdenum is calculated for different disruption energies and different energy fluxes.

The duration of melting, which is an important factor in determining the melt layer stability under different forces, is calculated for both stainless steel and molybdenum. The duration of the melt layer may in fact be shorter for materials with thicker melt layers. The effect of vapor shielding (the stopping of the incoming plasma ions by the vaporized wall material) on the dynamics of melting is also investigated.

1. Introduction

Plasma disruptions in tokamak devices are expected to deposit large amounts of energy in a relatively short time. This causes the first wall that is exposed to the energy deposition to be heated excessively such that melting and evaporation may occur. For large tokamak devices such as FED or INTOR, melting and evaporation may then contribute to the wall erosion. A comprehensive computer code has recently been developed at the University of Wisconsin to investigate the thermal response of a first wall component in the course of a plasma disruption. In a previous paper [1] the authors reported on the maximum thickness of the first wall material which evaporates and which melts. It was found that there exist threshold values for the density of energy deposited above which melting and evaporation become significant. As one would expect, the threshold value for melting is lower than that for evaporation. However, for very short disruption times, the two threshold values do not differ greatly. As the disruption time increases, both energy flux threshold values increase as well as the difference between the two. Whereas a longer disruption results in less evaporation for a fixed amount of energy deposited, the same cannot be said about the melt layer thickness. This is particularly true when the deposited energy is substantially above the threshold for melting; in these cases longer disruption times result in more melting.

The extent of the erosion of the first wall as a result of plasma disruption depends not only on the amount of material vaporized, but also on the melt layer stability [2]. If part or all of the melt layer were removed, the wall erosion due to plasma disruptions could be dramatic. One of the important factors which determines the melt layer stability is the duration of the molten state. Furthermore, the melt thickness will also influence the stability, so that it is important to know what fraction of the first wall thickness is in the liquid state for what period of time. This requires a precise evaluation for the dynamics of melting, evaporation and resolidification following a plasma disruption, the object of this paper.

2. Time and amount of energy deposition

Since the exact cause and the dynamics of hard plasma disruptions are still unknown, there is much uncertainty about the location, the amount, and the duration of the energy deposition. Therefore, only estimates can be provided for these parameters and they cover a substantial range of values.

The hard plasma disruptions are currently thought to involve two time periods, the thermal quench period followed immediately by the current decay period. The latter is estimated to be about twice as long as the first period. During the thermal quench, the plasma thermal

0022-3115/82/0000-0000/$02.75

Table 1
Range of disruption parameters for proposed tokamak reactors

Reference design	FED [5]	INTOR [6]	STARFIRE [7]
Plasma thermal energy (MJ)	109	244	1050
Stored magnetic field energy (MJ)	61	94	361
Total stored energy (MJ)	170	338	1411
First wall area (m^2)	366	380	780
Thermal quench time (ms)	5	to	20
Estimated range of energy flux during thermal quench (J cm^{-2})	90–650	200–1400	400–2800
Current decay time (ms)	10	to	40
Energy flux during current decay time (J cm^{-2})	60	90	170

energy is deposited on a certain fraction of the first wall, normally on the inboard side. Part of the thermal energy is however dissipated as X-rays, and therefore uniformly distributed over the first wall. During the current decay period, the stored magnetic energy is in part dissipated as ohmic heating of the first wall by eddy currents. Assuming that 50% of the magnetic energy is deposited in this manner, we have calculated the value of the energy fluxes in several proposed tokamaks (table 1). Because of the uncertainty of the area hit by the plasma ions, the uncertainty in the thermal quench time, and the uncertainty in peaking factors, the values for the thermal energy flux vary over the large ranges given in table 1. In the present study we have therefore considered values for the total energy deposition in the range from 325 to 1200 J cm^{-2}. Disruption times of 5 and 10 ms were assumed, though most of the results presented here will be for the shorter disruption time of 5 ms. It should be noted that these values were chosen mainly for purposes of illustrating typical time dependencies of the melt layer duration and the temperature history.

3. Thermal response model

The evaluation of the time and space dependent temperature distribution through the first wall component exposed to the hard plasma disruption is accomplished with a finite-difference computer code described previously [1,3]. The thermophysical properties of the solid and liquid phase of the first wall material are allowed to vary with the temperature. The back surface of the wall is assumed to remain at a constant value of the coolant temperature during the disruption, although a variable temperature or a different boundary condition can be treated if so desired. However, due to the thermal inertia of the first wall, the present assumption is well justified.

In the course of heating the first wall by a given heat flux from the plasma side, the temperature history follows a pre-heat period until the surface reaches the melting point. After this period, a moving-boundary problem is solved involving both the receding liquid surface and the changing liquid–solid interface. As described previously [1,3], this is accomplished in a coordinate frame moving with the liquid surface position. The boundary condition at the liquid surface is given by

$$F(t) = -k_l(\partial T/\partial x)|_{x=s(t)} + \rho_l(T_V)\, L_V v(T_V) + \epsilon_l \sigma\left(T_V^4 - T_0^4\right), \quad (1)$$

where $F(t)$ is the heat flux into the first wall at time t, $s(t)$ the position of the liquid surface at time t, k_l is the thermal conductivity of the liquid, ρ_l its density, ϵ_l its emissivity, σ is the Stefan–Boltzmann constant, $v(T_V)$ is the velocity of the receding surface, and L_V is the latent heat of evaporation. The first term in eq. (1) represents the heat conducted into the melt layer, the second term is the power dissipated in the evaporation, and the third term is the radiative heat transfer between the liquid surface and the colder portions of the first wall in direct line of sight. The velocity of the receding surface is related to the evaporation flux, and given by

$$v\left[T_V(t)\right] = \Omega J^{eq}\left[0.8 + 0.2\exp(-t/\tau_R)\right] \quad (2)$$

where Ω is the atomic volume for the first wall material and

$$J^{eq} = (2\pi M k_B T_V)^{-1/2} P_0 \exp(-\Delta H/k_B T_V) \quad (3)$$

is the equilibrium evaporation flux into a vacuum. Here M is the mass per atom, k_B the Boltzmann factor, P_0 and ΔH are materials constants for the equilibrium

vapor pressure [4], and T_V is the surface temperature. Eq. (2) contains a correction factor for the recondensation of vapor atoms on the melt surface, where τ_R is related to the collision time of vapor atoms.

The energy flux $F(t)$ may vary with time for two reasons. First, the dynamics of the plasma disruption will in general give a time-varying energy deposition rate. However, as little is known about these dynamics, most calculations were performed assuming a constant heat flux for a fixed disruption time. For comparison purposes, a triangular heat pulse was also considered.

The second cause of a variation in the heat flux $F(t)$ is due to the interaction of the plasma ions with the vapor emanating from the first wall surface. Collisions between plasma ions and vapor atoms lead to ionization and excitation. The amount of thermal plasma energy stored temporarily in the metal vapor may subsequently be dissipated in a more isotropic manner, and thereby reduce the energy flux. Although the details of this vapor shielding remain to be explored, an estimate of its effect on reducing $F(t)$ has been made previously [1] based on the following argument. The incoming plasma ions will be stopped in the condensed material within a certain range R depending on the ion energy and the energy stopping power of the first wall material. Neglecting any differences in the stopping power for solid, liquid, or gas, the ions will be stopped entirely in the vapor if the thickness of evaporated material is equal to R. The vapor is then assumed to re-emit the deposited ion energy instantaneously in an isotropic fashion, with only half of the energy reaching the first wall exposed to the plasma disruption. If the evaporated thickness $\Delta x(t)$ is less than R, the fraction of energy re-emitted by the hot vapor is only $F(t)[1-\Delta x(t)/2R]$.

4. Results

First wall materials considered in this study are type 316 stainless steel and molybdenum, and the thermophysical properties are those used in previous work [1,3]. For a constant heat flux maintained during the disruption time, the surface temperature varies in a characteristic manner illustrated in fig. 1. At the start of the disruption, the first wall temperature rises very rapidly until the melting point is reached. This defines then the pre-heat time and the start of melting. As energy is now consumed for further melting, the subsequent rate of surface temperature increase is slightly reduced for a short time. This can be discerned by an inflection point in the temperature rise curve. However, since the latent heat of fusion is not large, the inflection

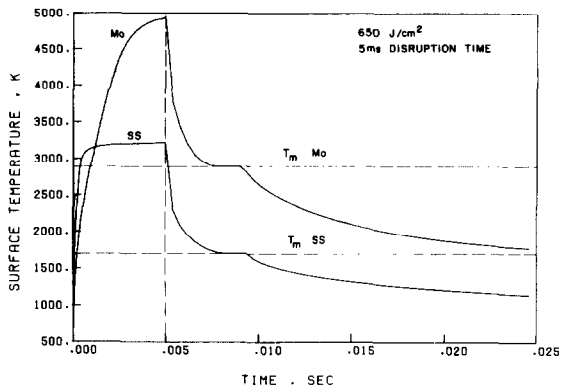

Fig. 1. Comparison of surface temperature rise for stainless steel and molybdenum for energy density of 650 J cm^{-2} and 5 ms disruption time (no vapor shield).

point is barely noticeable in fig. 1. As the surface temperature of the melt layer continues to rise, an ever-increasing fraction of the power input is consumed in evaporation as well as radiation. Hence the rate of temperature rise decreases rapidly until an equilibrium surface temperature is approached. For short disruption times, low energy fluxes, or materials with high melting point, the equilibrium temperature may never be reached. As fig. 1 shows, this is the case for molybdenum for the conditions illustrated. However, the stationary temperature is approached for the case of a stainless steel first wall. A close inspection of the surface temperature for stainless steel reveals, however, that it continues to rise at a very slow rate. The reason for this slow rise is that the melt interface moves into the solid material at a speed much larger than the velocity of the receding liquid surface. With the increasing melt layer thickness, the temperature difference between the melt surface and the melt–solid interface must increase in order to maintain the heat flux into the material required for further melting.

As the energy flux ceases, the surface temperature drops rapidly and approaches the melting point. Thereafter, it remains constant and equal to T_m until the melt layer has completely solidified. Then, the surface temperature resumes its decline. The melt duration, i.e. the period between the pre-heat time and the time for resolidification to occur, exceeds the time period of energy deposition by a significant amount. This melt duration is, however, affected by the time dependence of the heat flux.

Fig. 2 gives a comparison between a constant heat flux and a variable one in the form of a triangular time pulse. In both cases, the duration and the total energy

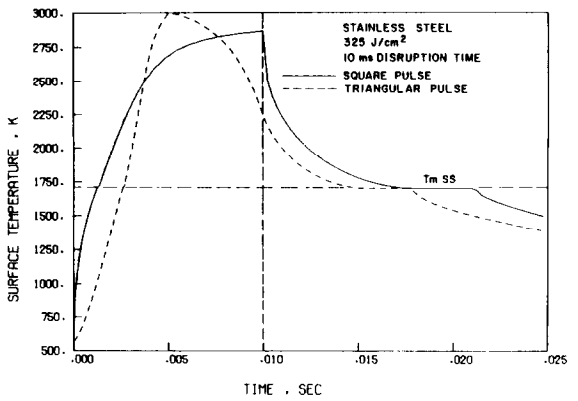

Fig. 2. Comparison of stainless steel surface temperature rise for square and triangular heat pulse shape.

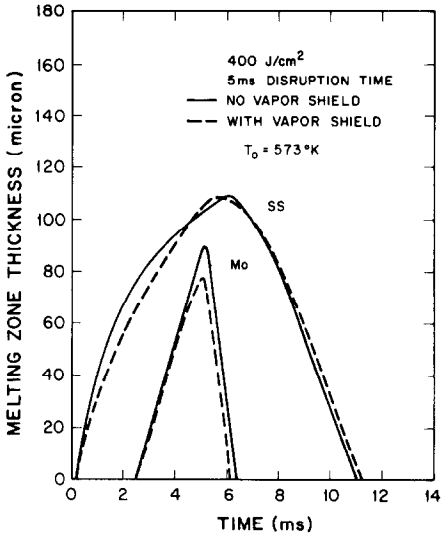

Fig. 3. Time dependence of melting zone thickness for stainless steel and molybdenum for 400 J cm^{-2} and 5 ms disruption time.

deposition are the same. It is seen that the square pulse deposition yields a substantially larger melt duration, but a lower maximum surface temperature. Conversely, a triangular pulse deposition gives shorter melt times, higher surface temperatures and somewhat larger values of integral evaporation. In fact, for the particular case shown in fig. 2, the triangular pulse deposition results in about 25% more material evaporated compared with the square pulse deposition, but the maximum melt layer thickness is reduced by about 15%. Therefore, it can be seen that the time structure of the disruption energy flux may be quite important.

The possibility of melt layer removal depends on many factors, including the force exerted by gravity, magnetic loads, and mechanical vibrations. In addition, however, the melt layer thickness and duration are of primary importance in any consideration of the melt layer stability and the question of in-situ resolidification.

Fig. 3–6 show the results of an extensive analysis of the melt layer evolution. For low values of energy deposition, vapor shielding has little effect on the melt layer formation as can be seen from fig. 3. With little evaporation taking place, this is an obvious result. At intermediate energies, however, vapor shielding may either increase or decrease both the amount and the duration of melting. Fig. 4 gives a clear demonstration of this latter effect. Vapor shielding reduces the total amount of energy deposition and hence the maximum surface temperature reached. For a material with high melting point, both evaporation and melting are then reduced, whereas for materials with lower melting point, the reduction in evaporation makes more energy available for conduction into the wall with subsequent melting.

The results shown in figs. 3 and 4 highlight an additional difference in the melt behavior of materials with medium and high melting temperature. In the case

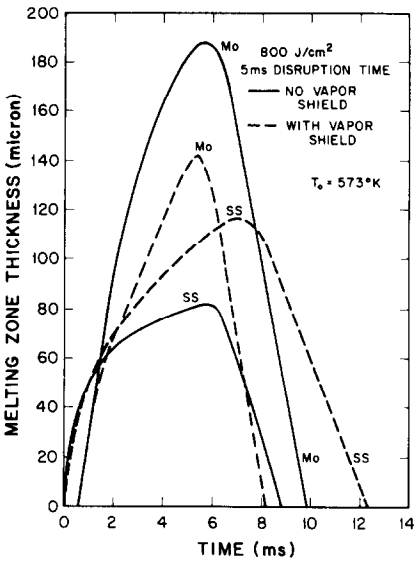

Fig. 4. Time dependence of melting zone thickness for stainless steel and molybdenum for 800 J cm^{-2} and 5 ms disruption time.

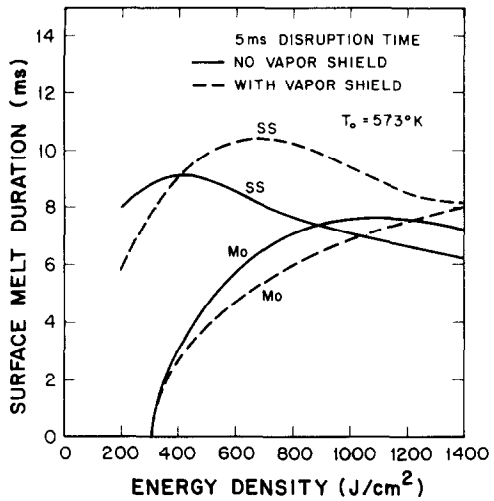

Fig. 5. Duration of surface melting as a function of energy deposited for both stainless steel and molybdenum.

of molybdenum, the melt layer thickness ceases to expand almost immediately after the energy flux drops. In contrast, melting continues for stainless steel for up to 1 ms after the disruption time. The thermal energy stored in the melt layer is sufficient to cause further melting as the heat is conducted into the material.

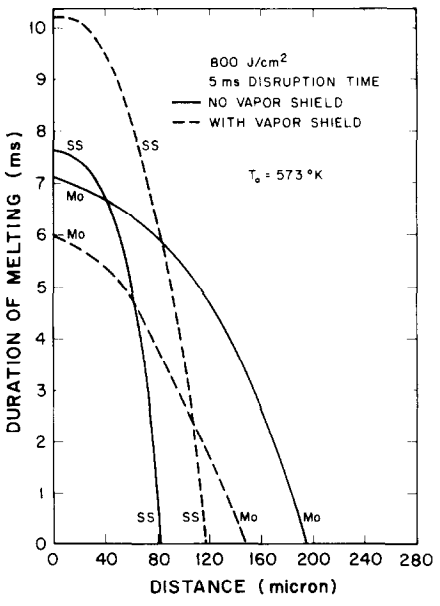

Fig. 6. Space dependence of duration of melting for stainless steel and molybdenum for 800 J cm^{-2} and 5 ms disruption time.

Other noteworthy features of the above results are that whereas stainless steel melts more than molybdenum for low values of energy deposition (fig. 3), the reverse is true for high energy depositions (fig. 4). This behavior is due to the fact that at high energy deposition, most of the energy goes into evaporation leaving a smaller fraction of the energy to be conducted into the material and cause melting. A corresponding reversal of the melt duration is further illustrated in fig. 5. Here, the time during which molten metal is present is shown as a function of energy deposition. For lower values of energy fluxes, when stainless steel melts more than molybdenum, the surface melt duration is longer for the material with lower melting point. At high energy fluxes, the melt duration is in fact longer for the material with higher melting point.

The duration and the thickness of the melt layer can be obtained from the complete temperature history, and it is shown in condensed form in fig. 6. The results display some interesting if not unexpected features. First, the melt layer thickness remains remarkably close to the maximum value. In other words, the rate of resolidification is at first very slow, but then accelerates rapidly. This is particularly true for stainless steel, and it indicates the resolidification occurs at a substantial rate only after the temperature in the entire melt layer has dropped to values close to the melting point. Second, although molybdenum exhibits more melting at medium energies than stainless steel, melt duration is shorter.

5. Discussion

The thermal response of a first wall component exposed to a hard plasma disruption can be accurately predicted if the rate of energy deposition is known. Unfortunately, the causes of the disruption and the subsequent behavior of the plasma are not well understood at the present time. Therefore, the response of and the consequences to the first wall components, such as limiters and divertor throats, must be assessed based on worst-case assumptions. The present computational model can serve as an important tool in component design and in material selection. The results discussed in the present paper on the dynamics of melt layer formation and resolidification together with the previously reported results on evaporation [1] clearly demonstrate that there is no simple criterion for an optimal choice of materials. Materials which are relatively immune to vaporization may exhibit more extensive melting. On the other hand, the duration of the melt layer may in

fact be shorter for materials with thicker melt layers. The fundamental reason for these diverging trends can be traced to the nonlinear dependence of the energy dissipation mechanisms such as heat conduction, melting, evaporation, and radiation, on the amount and duration of the plasma energy deposition, and to the interdependence of these mechanisms.

Acknowledgements

Partial support for this work has been provided by the Japan Atomic Energy Research Institute (JAERI) and by the Wisconsin Electric Utilities Research Foundation (WEURF).

References

[1] A.M. Hassanein, G.L. Kulcinski and W.G. Wolfer, J. Nucl. Mater. 103/104 (1981) 321.
[2] W.G. Wolfer and A.M. Hassanein, these proceedings.
[3] A.M. Hassanein, G.L. Kulcinski and W.G. Wolfer, Nucl. Fus. (submitted).
[4] A.M. Hassanein, Ph.D. Thesis, Univ. of Wisconsin – Madison (1982) (UWFDM-465).
[5] C.A. Flanagan, D. Steiner and G.E. Smith, Oak Ridge Nat. Lab. Rep. ORNL/TM-7948.
[6] INTOR – US Contribution to the International Tokamak Reactor Phase-1 Workshop, USA INTOR/80-1 (June 1980).
[7] STARFIRE, Argonne Nat. Lab. Rep. ANL/FPP-80-1 (1981).